CsI Time Resolution Study with Custom Built Digitizer for the KOTO Experiment

Emily Casey
Advisor: Yau Wah
Co-Reader Jiasen Ma

May 12, 2012

1 Abstract

The purpose of my thesis experiment is to measure the time resolution of the cesium-iodide scintillator crystals with custom built analog-to-digital-converter boards (ADCs) for the KOTO experiment. Simulation shows that the time resolution should be better than 0.50ns when the energy deposited is above 10 MeV and better than 0.15ns when the energy deposited is above 200MeV. Over time, my thesis diverged into two parts. The first part, the test bench, is a more elaborate and versatile setup involving an array of 16 CsI crystal and two wire chambers. I have made steady progress on the test bench but it is not yet producing meaningful data. In part two of my research I tested the time resolution of the ADC boards using a pared down setup involving two CsI crystals. The time resolution for high energy cosmic muons event was $0.599 \pm 0.015\text{ns}$. This time resolution is greater than what we would expect for the cosmic muon events we were measuring (each muon deposits approximately 20 MeV). I investigated several possible factors affecting the time uncertainty in this setup including the position of the muon track within the crystal (and the resultant pattern of light dispersion), the mean number of photoelectrons per event, and the uncertainty in position. I identified the number of photoelectrons per pulse the primary factor limiting time resolution. This experiment also demonstrated that there can be considerable variability in photoelectron statistics between different CsI crystals. This has important implications for the KOTO CsI array. The photoelectrons per MeV for each block should be measured individually in order to truly understand calorimeter performance.

2 Theory

2.1 Larger Context

The goal of the KOTO experiment is to measure the probability with which neutral kaons decay via the golden decay mode,

$$K_L \rightarrow \pi_0 \nu \bar{\nu}$$

This decay mode is of interest because it is an instance of direct CP Violation. CP symmetry is the invariance of a physical process under both charge and parity reversal. In simple terms, CP symmetry implies that if all particles are exchanged with their anti-paritcles, and all spatial coordinates are mirrored, the system behavior should not change. When this principal is broken, we say that CP symmetry has been violated. The Standard Model predicts that the branching ratio of the golden decay should be $2.8 \pm 0.4 \times 10^{-11}$. However, models such as supersymmetric theory predict different branching ratios for this decay. Therefore, directly measuring the branching ratio will either validate the Standard Model or open up room for new physics while providing an important check on alternative theories. The KOTO experiment hopes to measure this branching ratio with an uncertainty less than 10%. The CP Violation group at Chicago is in charge of creating the electronics for the KOTO experiment.

The pion from the golden decay decays quickly into two gamma ray photons. The KOTO detector uses a CsI calorimeter to detect the position and energy of the photons as they strike the back of the main barrel. Using the position and energy, the decay vertex is reconstructed and the transverse momentum of the pion is determined.

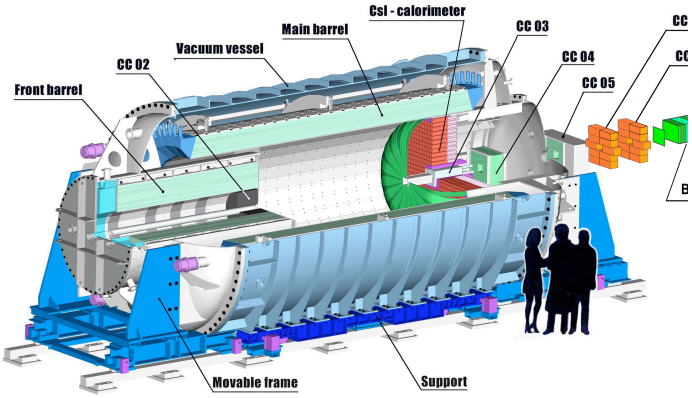

Figure 1: KOTO Detector

The CsI Crystals emit light with energy proportional to the energy deposited by the photons. Light from each CsI scintillator crystal strikes the photocathode of a photomultiplier tube where each photon causes an electron to be ejected via the photoelectric effect. Then, the electrons are accelerated through a series of dynodes which amplify the signal. The ADC boards reshape this signal and record the time and amplitude of the pulse as described above. It is critical that the boards have good time resolution so that two photons arriving in quick succession are not mistaken for single photon of higher energy. This mistake could lead experimenters to believe that only two gammas were produced when this was not actually the case. This could lead to false identifications of the golden decay.

The curved side of the main barrel of the KOTO detector is fitted with a charged particle veto. The purpose of the veto is to exclude events that result in more than two gammas, but only two of which actually hit the calorimeter. The more accurately we can measure the arrival time of signal gammas the more precisely we can define the time window during which a veto can occur. A smaller veto window results in a larger total acceptance, which is of premium importance when trying to observe a decay with such a low branching ratio. Thus, the time resolution of the ADC boards is of critical importance for improving the acceptance of the detector.

2.2 About the ADC Boards

A CsI PMT pulse has a sharp leading edge followed by a long tail. The ADC boards for KOTO employ a ten-pole filter to reshape CsI pulses into quasi-gaussian pulses.

The ten-pole filter consists of 5 capacitors and 5 inductors. The filtered pulses are sampled by a 125MHz flash ADC. The ADC begins sampling when the global trigger arrives, and takes 96 measurements per trigger. The voltage is recorded in units called counts which are linearly related to voltage. When analyzing ADC data we subtract the pedestal (the baseline counts recorded when the voltage is zero) graph the ADC output (counts vs. time) and fit the data to a gaussian shape using the least-squares method. We define the time of arrival of the pulse to be the mean time of the gaussian pulse.

The time resolution of the measurement should be ten times better than the time resolution that can be achieved with standard TDC technology. Because a pulse takes place over a finite window of time, we must pick specific pointlike feature along the pulse shape and define the time of that point to be the time of the pulse. Typically the rising edge of an unshaped scintilaltor pulse is the feature used to define time. A TDC measures the time of the leading edge by emitting a square pulse when the voltage crosses a certain threshold. The time of arrival of the pulse is defined to be the time of the leading edge of the emitted square pulse. However, because the leading edge of the scintillator pulse is not perfectly vertical, the point where the voltage crosses the threshold value will be closer to beginning of a pulse of larger

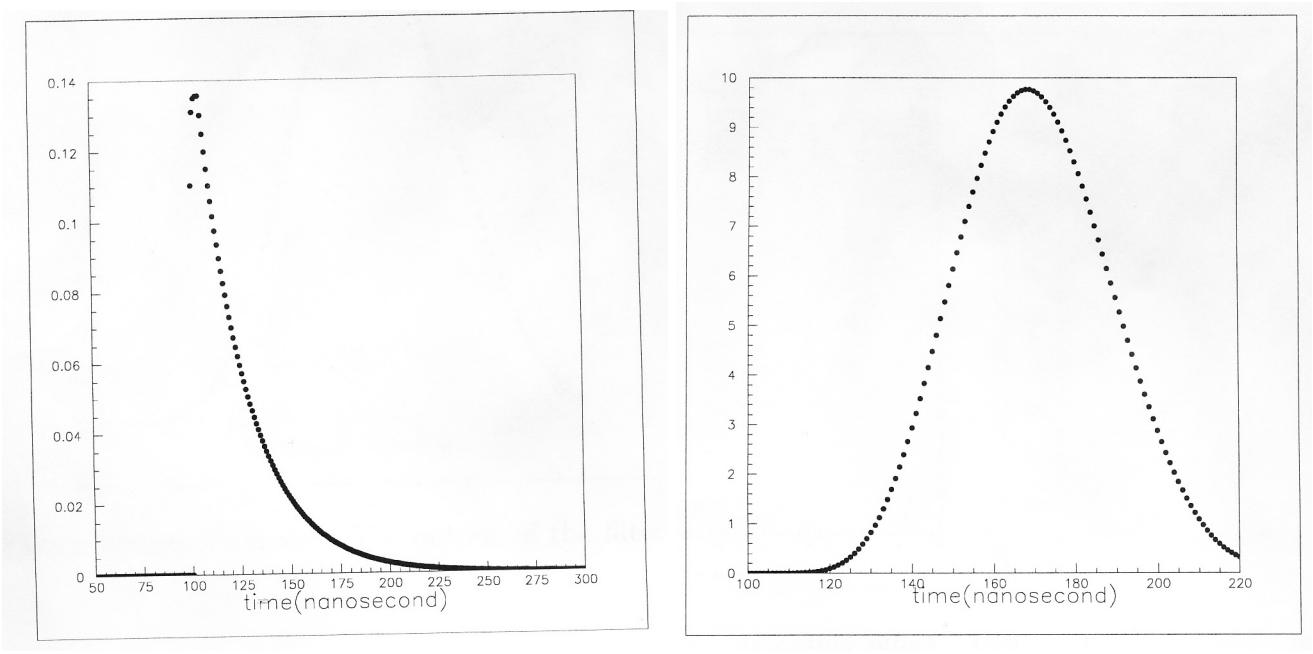

Figure 2: Monte-Carlo Simulation of CsI Pulse Before (Left) and After (Right) Reshaping

amplitude(in proportion to its length) than a pulse of smaller amplitude. This means that when we measure the time of arrival of pulses of different amplitudes we are actually meauring slightly different points along the lengths of the pulses, resulting in an inherent timing unceirainty.

The filter reshaping results in superior time resolution because each pulse is made symmetric and gaussian in a deterministic way. Unlike the rising edge of a scintillator pulse, the mean of a gaussian pulse is ideally pointlike. Because the pulses produced by our filter are not all perfectly gaussian, there is some uncertainty in time that results from pulse shape, but this effect is small compared with the timing uncertainty using standard TDC technology. With many points taken on both the rising and falling edges of the pulse, the mean time of the peak can be determined quite accurately. The predicted superiority of the time resolution was calculated by the CP Violation group using a Monte-Carlo simulation (Ma 2007).

3 Apparatus

High energy particles are needed to test the time resolution of the ADC boards in the relevant range of scintillator pulse energies . Because cosmic rays are conveniently available high energy particles, our group decided to create a test bench that utilized cosmic muons to test the ADC boards. Figure 3 displays a schematic of the test bench. Cosmic muons travel in a direction that is generally perpendicular to the ground. We have vertically sandwiched an array of CsI crystals between two wire chambers. The wire chambers allow us to pinpoint with high precision two spatial points through which a muon passes. We draw a straight line between these paths and assume that this is the muon trajectory through the CsI array (coulomb forces acting on the muon do create slight deflection resulting in a path that is not perfectly linear but this deflection is negligible given the spatial resolution of our experiment). For muons of a given trajectory, we then examine the CsI data and characterize the spread in pulse times. Plastic scintillators at the bottom of the bench are used to identify muons and trigger data taking. The scintillators are shielded by lead. Because cosmic muon have a long attenuation length in lead compared to other cosmic particles, the lead ensuring a clean high energy muon signal.

3.1 Triggering

The plastic Scintillators at the bottom of the apparatus are used to trigger data taking. All three signals are discriminated and then fed into a logic unit. Data taking is only triggered when all three scintillators are in coincidence. The plastic scintillator signal will be used to define time 0 when calculating drift time for wire chamber events.

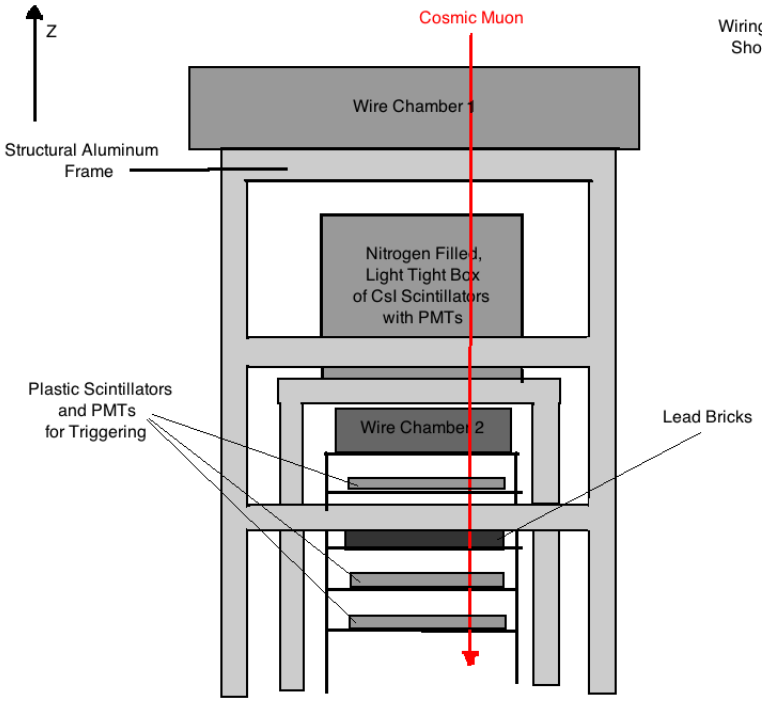

Figure 3: Cosmic Ray Test Bench

3.2 Drift Chambers

A drift chamber is composed of stacked planes of parallel wires. Wires held at negative high voltage wires (approximately -2000 V) alternate with grounded wires. Each grounded wire constitutes one channel of signal. Each chamber is composed of four such planes. In two of the planes the wires run parallel to the x direction and in the other two planes the wires run parallel the y direction. The entire chamber is sealed from the atmosphere and filled with a mixture of argon and carbon-dioxide gas. The argon-carbon-dioxide gas allows the wire chamber to operate at -2000V. At this voltage regular air would ionize and create current. When a charged muon passes through the drift chambers it ionizes gas molecules as it travels. The resulting electrons are pushed towards the nearest grounded wire by Coulomb forces. When an electron gains enough energy it ionizes another gas molecule. This process repeats, resulting in an electromagnetic shower propagating in the direction of the nearest grounded wire. Finally, the electrons reach the grounded wire and the signal is amplified and recorded. The shape of the shower is such that it creates a negative pulse with a sharp leading edge and a long tale. The gas is carefully chosen so that electrons reach terminal velocity quickly and thus, on average, travel at a relatively constant speed towards the grounded wire. The drift time is defined to be the length of time between the when the muon enters the chamber and the time the beginning of the shower arrives at the wire. The drift time, the drift velocity, and the location of the wire which records the signal are used to reconstruct the position of muon in the x and y directions with 100μm precision. The planes with wires running along x axis are used to determine y position and vice versa. Two planes in each direction are necessary in order to resolve ambiguity as to which side of the signal wire a shower orignates on. The two planes are offset by one half cell (a HV wire is located direction below a grounded wire and vice versa) and therefore the pair of wires that receive signal together determine the position. The wire geometry is illustrated in figure 4.

The output signal from the grounded wire is first amplified using a pre-amplifier card. Then it is converted to differential signal and sent to a 500 MHz board to be digitized (without reshaping).

3.3 CsI Scintillators

The scintillators are contained in an aluminum box filled with nitrogen continually created by a nitrogen generator (it uses a molecular sieve to separate nitrogen from the other components of air). The nitrogen is necessary because the crystals are slightly hygroscopic and could be damaged by water in the air. Filling the box with pure nitrogen is a convenient way to ensure the gas in the box is dry. Muons passing through the CsI scintillators are slowed and deflected slightly by coulomb

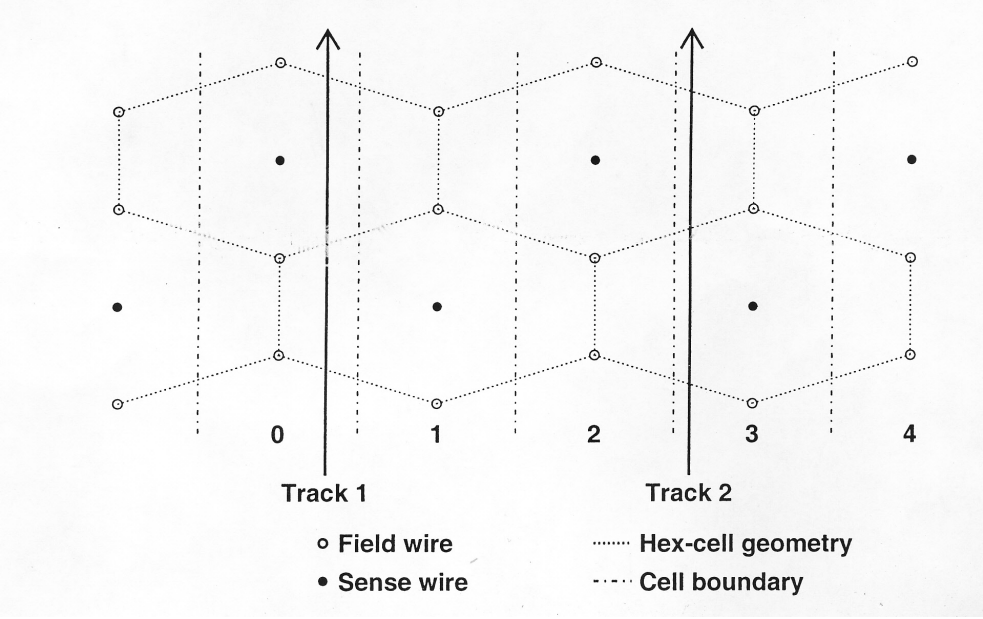

Figure 4: Wire Chamber Cell Geometry

forces between the muons and protons and electrons in the crystals. The deceleration results in Bremsstrahlung radiation. The crystals convert the energy radiated by the muons into light. The light from each scintillator crystal strikes the surface of a photomultiplier tube where an electrons are ejected via the photoelectric effect. Then the electrons are accelerated through a series of dynodes which amplify the signal. Thus the signal from the PMT tubes are negative pulses with a sharp leading edge and a long tail. These pulses are sent to ADC boards which reshape and sample the pulse as described above

3.4 Data Aquisition

Signals from the plastic scintillators are discriminated and sent to a coincidence unit. The output from the coincidence unit is converted to LVDS form which is then sent to the MT board. The MT board is a special board that keeps the global clock and passes the clock and the trigger signal to the ADC boards. Each ADC board has 16 channels. Input to the ADC must be a differential signal so CsI data signals are sent to special boards that convert from 50 ohm to differential signal and the output from those boards is then sent to the ADC input. ADC boards are are controlled by a VME controller which receives instructions from a PC. The PC receives and stores the data.

4 Progress

4.1 Preparing the Wire Chambers

One of the drift chambers we used (the upper chamber) is from the KTeV experiment. I have hooked this chamber up to gas canister and so that it is constantly filled with argon-carbon-dioxide gas. Initially, the chamber high voltage could not be increased beyond -600V without drawing too much current and causing the voltage supply safety mechanism to turn the voltage off. My best guess is that this behavior was caused by dust that had accumulated in the chambers over years of disuse. Slowly, over the course of few weeks, I turned up the high voltage 100V per day until it finally was able to maintain -2000V while drawing only approximately 0.5 μA current. Now, after months of running at 2000V the current is at an all time low of 0.1 μA .

After the desired voltage was achieved I I helped to add an aluminum support to the edge of the chamber supporting the pre-amp cards to that the cables carrying the signal from each chamber channel to the 500 MHz boards could be attached without the weight of the cables putting force on the edge of the pre-amp card that plugs into the chamber. These cables have been mounted on wire racks that lead into the DAQ room. Here I attached the cable to boards that amplified the

signal 5 times. Then I sent the output from the amplifiers to another board that converted differential signal back to 50 ohm so that I could look at the amplified signal from each channel on the scope and verify that the data transmission and amplification was achieved without issue. Then I began the process of verifying that all chamber channels were functional.

I used an x-ray source and an oscilloscope to observe the signal leaving the pre-amplifier. The x-ray photons interact with the chamber gas via the photoelectric effect, producing single electrons. These electrons result in electromagnetic showers, albeit smaller than those produced by the ionization track of the muons. For most channels I observed the expected negative pulses. However, approximately 20% of channels displayed constant voltage oscillations regardless of whether or not the source was present. My best guess as to the source of the oscillations was that they were caused by competing grounds. However, efforts to solve the problem by floating some equipment and by adding connections between grounds have produced no improvement.

Next I began looking for signal from cosmic muons on each wire. Most of the non-oscilating wires displayed a clear cosmic signal but roughly 10% of the wires seemed to be preforming with poor efficiency. These wires appeared to be hit only one fifth as often as the others. Because we have good reason to believe the cosmic muons are passing through the chamber with a uniform spatial distribution, this low hit rate must be due to equipment malfunction.

Because we were unable to stop some of the chamber wire from constantly oscillating or to improve the efficiency of the low-rate wires, we eventually abandoned using the large KTeV wire chamber and added another small wire chamber to the apparatus, directly above CsI array, resting on the CsI box. We preformed the the same same x-ray source testing on this smaller chamber and observed the signal from each wire on the oscilloscope. All wires in this small chamber are behaving as desired.

The lower chamber I constructed with the help of two other undergraduates over the course of a month. We inherited the pieces of the frame from a previous experiment. We strung gold plated tungsten wires across the chamber, using lead weights to create appropriate tension. I secured the wires with epoxy and, soldered the wires to the frame. I attached the preamplifier cards to the chamber frame, and connected the different preamplifier input to the correct wires. Between each plane of wires was a streched sheet of aluminized mylar. I connected this mylar to the ground input on the preamplifier cards. Then I bolted the chamber together and sealed it with RTV.

After filling the chamber with gas, it held 2000V without problem. Unlike the larger chamber inherited from KTeV, the chamber I helped construct requires a positive high voltage source and the high voltage wires carry the signal. Testing with the x-ray source indicates that all of the chamber channels are working. All channels seem to be detecting cosmic signal at approximately the same rate.

4.2 Trigger Scintillator Plateaus

I have conducted tests to find the plateau voltages for the plastic scintillators. In order to do this I supplied two of the plastic scintillators with HV. I discriminated both of their outputs so that a square wave was produced when the scintillators emitted a pulse with amplitude above a certain threshold. I set up two counters. One counter records the number of events observed by one of the scintillators. The other counter recorded the number of coincidences. Then I slowly increased the High Voltage supplied to the scintillator (while keeping the voltage supplied to the other constant) and recorded the ratio of coincidences to events. When this ratio reached a plateau I chose this voltage to operate scintillator at. When all of the scintillators reached plateaus I wired them into a logic unit and used output as a trigger. The trigger signal was sent to a MT board which passed the trigger to two other MT boards. The MT boards passed the trigger along with the global clock to the ADC boards being used to digitize the scintillator signal.

4.3 CsI Array

I stacked the CSI crystals in an aluminum box and hooked each PMT to a high voltage supply. I attached the signal output from each PMT to the input of a 50Ω to differential signal converter and then attached the output from the convert to the input of an ADC board.

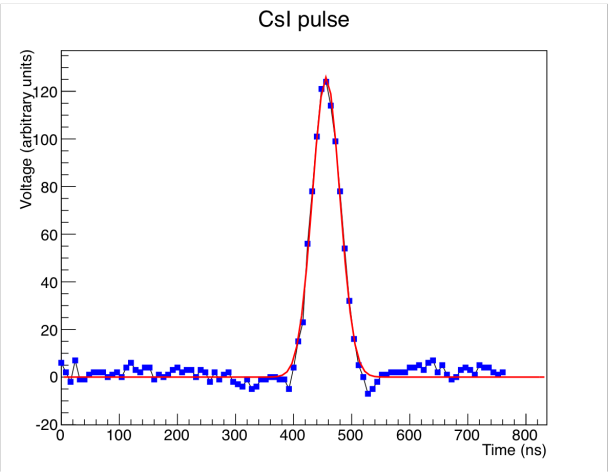

Figure 5: Reshaped CsI Pulse with Pedestal Subtracted

4.4 Test Bench Results

Using data from the CsI array and the two wire chambers we are able to reconstruct the paths of cosmic muons as they travel through the test bench. Right now we are only using the identity of the wires receiving signal to construct the muon path. After we calibrate the time offsets we will be able to use drift time to determine the track more accurately. We are working hard on the data analysis software now and hope to produce measurements of the time resolution within a month.

5 Small Trial Setup

While working on the test bench, I have concurrently been using a scaled down setup to investigate the time resolution of the boards. First, I used data from a single crystal to develop data analysis and pedestal subtracting software. Then I used this software to calculate the time resolution using a small apparatus consisting of one CsI crystal and four plastic scintillators. Then I added a second crystal to the apparatus, improved the measurements and investigated several factors affecting time resolution.

5.1 Looking at CsI Pulses

I took several runs of data with one separate CsI crystal and performed some preliminary diagnostics. First I checked that the pulses had the expected gaussian shape. Everything matched predictions. Then, using C++ and Root I created a program to read CsI events into an organized data structure, fit pulses, record whether the data did indeed represent a pulse (whether the voltage ever crossed a given threshold), and find the mean time and amplitude of all true pulses.

When I first began analyzing CsI data, I used pedestal values calculated from a specific pedestal run which was taken with the high voltage to the PMTs turned off to insure there was no signal. However, as I analyzed more data it became clear that the mean pedestal value changed slowly over the course of many events. Therefore I devised a new pedestal subtraction system that calculated the pedestal separately for each run being analyzed. A run is a group of 40 events and the data from each run is stored in its own file. Although a run is arbitrary quantity of events, it is convenient size for pedestal subtraction because the pedestal value never changed by more than one count in a run. Therefore, for each run I averaged the voltage values of the first ten samples from each event in the run and used this as a pedestal value. Because pulses never arrived within the first fourth of the event window I decided it was safe to assume that the first ten counts were representative of the pedestal. The standard deviation of the pedestal value never changed and remained at a constant 2.7 counts.

I used the standard deviation of the pedestal voltage as the vertical error bar my CsI pulse fitting program. A sample pulse after pedestal subtraction is provided below in Figure 6. The amplitude is in arbitrary units of voltage.

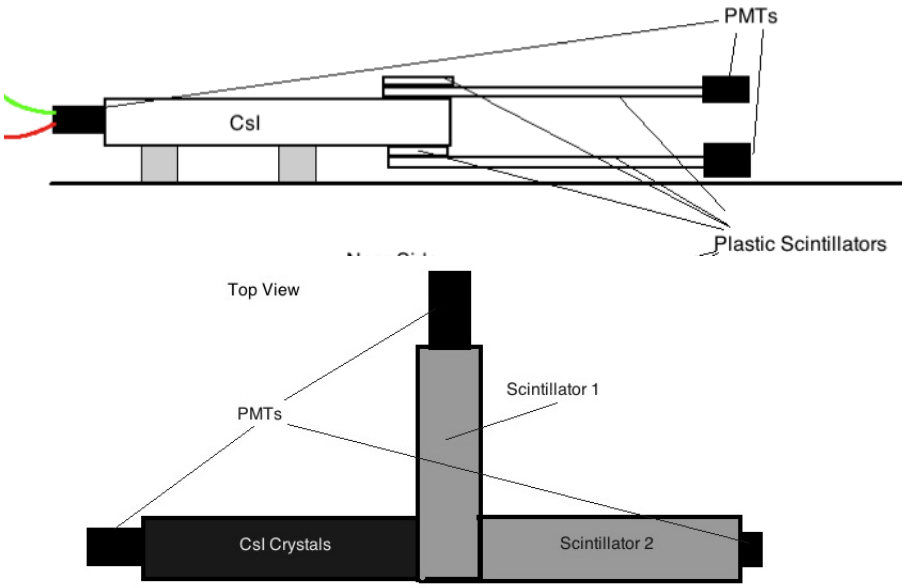

Figure 6: Single Crystal Setup

5.2 One Crystal Results

I began this investigation using one CsI scintillator and four plastic scintillators arranged as depicted in Figure 7.
The signals from the four plastic scintillators were each discriminated and then fed into a logic unit. The logic unit was set to 4-way coincidence. When all four discriminated scintillator signals produced overlapping pulses, the coincidence unit emitted a square trigger pulse (we measured the trigger rate to be approximately 1x per 5 minutes using a scalar count record incoming triggers over a 5 hour period). The output from the coincidence unit was fed into a lemo to ECL converter. The signal was then converted from ECL to LVDS and then sent to the ADC trigger input. Because of the limited amount of data being taken we only needed to use one ADC board (each board has 16 channels) and thus the trigger signal was sent directly to the ADC board instead of to the MT board. In the KOTO experiment and in the test bench, the MT board accepts the trigger signal and functions as a fanout passing the signal to multiple ADC boards. The MT board also passes the global clock to the ADC boards so that data taking is synchronized. Because there were no other boards to synchronize with we used the internal clock feature of ADC board, inputted the trigger signal directly and bypassed the MT entirely.

Each trigger should indicate a muon passing through the apparatus within a vertical column with 10cm x 10cm square cross sectional area. I wrote a program using C++ and Root to fit each pulse to a gaussian and record the mean time. Figure 8 is an example of one of the fitted pulses. The pedestal fluctuation defines the uncertainty in the y direction on each of the data points in Figure 8. The vertical error bars exist but are too small to be seen on the pulse in Figure 8.
A cursory visual inspection of 10% of the roughly 6000 events I collected with the single crystal setup indicated that the fitting program was producing sensical results. The average error that the fitting program reported, when calculating mean time of the pulse, was 0.30ns. This fit error places a lower bound on the acheivable time resolution.

After fitting each pulse to a gaussian I used the the of arrival of the pulse in the bottom plastic scintillator (Scintillator 4 in the diagram) to define t_0 (time=0). The time of arrival of the pulse in the bottom plastic scintillator was determined with the same ADC digitalization and fitting methods that we used to dertermine the time of the CsI pulse. Then, for each event, I subtracted the mean time of the CsI pulse from the time of the Scintillator 4 pulse.

After we fit the pulse to a gaussian shape, the mean time of the pulse indicates how many nanoseconds after the data taking began that the pulse arrived. Because we are assuming that all muons that trigger data taking are spatially identical, the difference in time between trigger arrival and pulse arrival should be the same for all events. However, The ADCs run on a 125MHz clock and data taking can only begin at the beginning of a clock cycle. Therefore depending on when the muon arrives temporally in relation to the clock cycle, there can be as little as 0 ns or up to 8 ns between

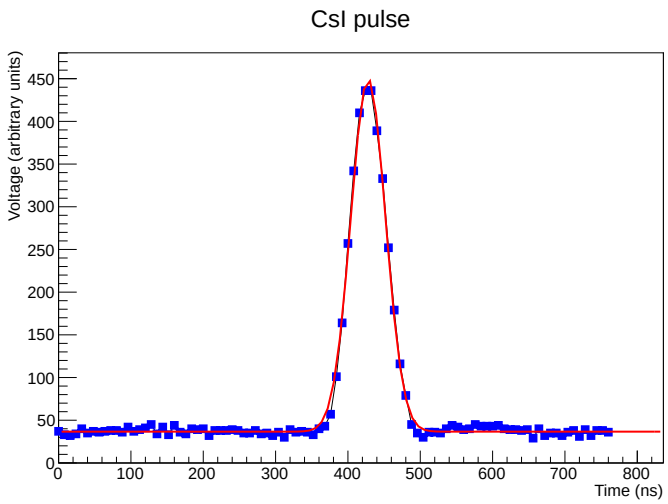

Figure 7: Reshaped and Digitalized CsI Pulse with Pedestal Subtracted

trigger and arrival and the first sample taken. Therefore the time of arrival of the pulse, counted in nanoseconds from the sample, has a random jitter built into it. This jitter results in differences in mean pulse time even when muons are spatially identical. Therefore it is necessary that we define a different t_0 than the first sample. Let us denote the time of CsI pulse arrival relative to the begining of data taking as t_{CsI}. If we take t_0 to be the time of arrival of the pulse in the bottom scintillator, then t_0 is affected by the same exact of trigger jitter that t_{CsI} is, therefore the difference between t_{CsI} and t_0 is unaffected by trigger jitter and should be the same for all spatially identical events.

$$t = t_{CsI} - t_0$$

Any variation in t is a result of imperfect time resolution. A histogram of the values of t over the course of 876 events is presented below.

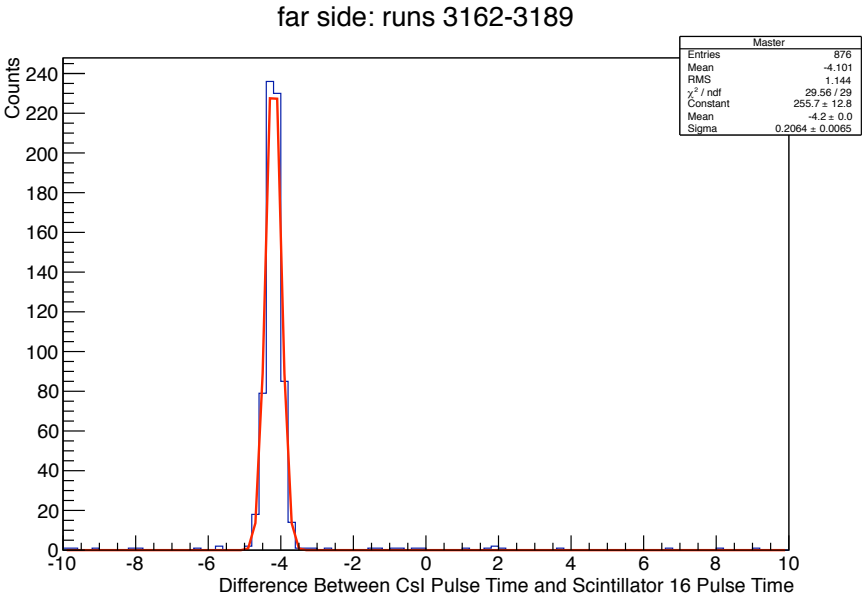

Figure 8: Histogram of Pulse Times for Single Crystal Setup

After fitting this histogram to a gaussian I found the standard deviation of the pulse time to be 0.2064 ± 0.0065 counts. Since the ADC takes 1 count per 8ns the standard deviation is $1.6515 \pm 0.052\text{ns}$. This time resolution is clearly much larger than desired.

5.3 Two Crystal Results

After taking these measurements it became clear that the role of the plastic scintillator in defining t_0 was reducing the accuracy of the timing. The ADC boards are specifically designed to reshape CsI pulses into gaussians, when they are used to reshape plastic scintillator pulses the output is less perfectly gaussian. If the pulses are less gaussian then there is a greater uncertainty in time resolution as described in the theory section of the paper. Because the pulse time t is defined relative to t_0 the time resolution of t is actually the result of the uncertainty in the measurement of t_{CsI} and the uncertainty in the measurement of t_0 added in quadrature.

$$t = t_{CsI} - T_0$$

$$\Delta t = \sqrt{(\Delta T_{CsI})^2 + (\Delta t_0)^2}$$

By adding a second CsI crystal we can make Δt_0 approximately equal to Δ_{CsI} and therefore Δ_{CsI} can be calculated rather than being overshadowed by the larger plastic scintillator resolution.

$$\Delta t = \sqrt{(\Delta t_{CsI})^2 + (\Delta t_0)^2} = \sqrt{2(\Delta t_{CsI})^2}$$
$$\Rightarrow \Delta t_{CsI} = \frac{\Delta t}{\sqrt{2}}$$

Below is a picture of the revised setup.

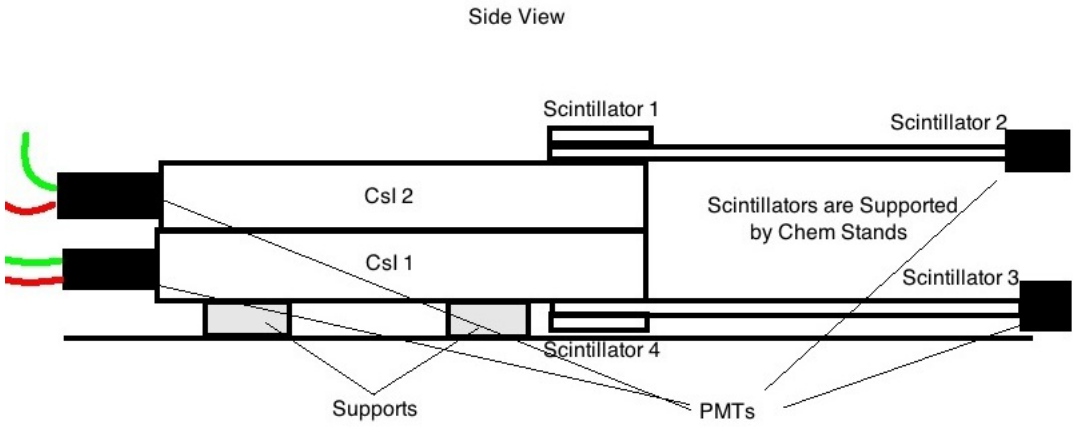

Figure 9: Two Crystal Setup

Figure 11 is a histogram of t for data taken with this 2 crystal setup.

After fitting the histogram to a gaussian we find the standard deviation of the event times to be

$$\sigma = 1.196 \pm 0.020.$$

This indicates that the time resolution of a single CsI pulse time, σ_{CsI} is

$$\sigma_{CsI} = \frac{\sigma}{\sqrt{2}} = \frac{1.196}{\sqrt{2}} = 0.846$$

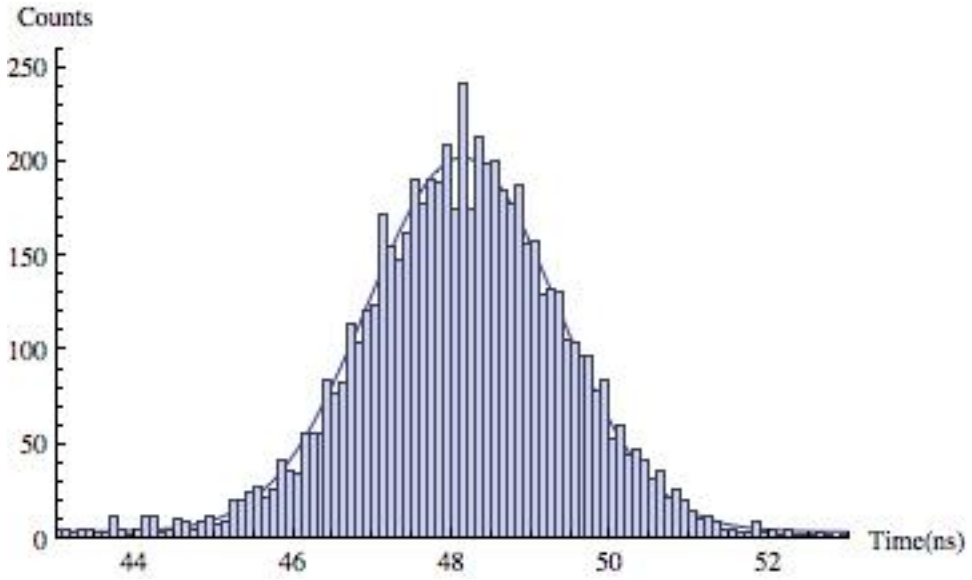

Parameter	Fit Estimate	Standard Error
Amplitude a (counts)	594	11
Mean μ (ns)	48.125	0.016
Standard Deviation σ (ns)	1.19	0.02

Figure 10: Histogram of Pulse Times for Two Crystal Setup and Fit Statistics

Now we calculate the error in this quantity.

$$\Delta\sigma_{CsI} = \frac{\partial\sigma_{CsI}}{\partial\sigma}\Delta\sigma = \frac{0.020}{\sqrt{2}} = 0.014$$

We see that the time resolution $\sigma_{CsI} = 0.846 \pm 0.014$, which is still greater than desired. We would like the time resolution to be less than 0.5ns because the energy deposited should over 10MeV.

Next I investigated whether the end of the crystal that the muon traveled through and thus the resulting way in which the light scattered into the photocathode affected the time resolution. I rearranged the CsI 2 as shown below so that the muon passed through the end of the crystal near to the PMT.
As indicated by table and histogram below there was no significant difference in time resolution.
However, a significant increase in time resolution was acheived when a different CsI crystal and PMT were used. We will call this new crystal CsI 3. Although the crystal and phototube were supposed to be identical to the original pair, the time resolution was significantly better.
Using the data taken with CsI 3 we calculate the following time resolution.

$$\sigma = 0.977 \pm 0.011.$$

$$\sigma_{CsI} = \frac{\sigma}{\sqrt{2}} = \frac{0.977}{\sqrt{2}} = 0.691$$

$$\Delta\sigma_{CsI} = \frac{\partial\sigma_{CsI}}{\partial\sigma}\Delta\sigma = \frac{0.011}{\sqrt{2}} = 0.008$$

so,

$$\Delta\sigma_{CsI} = 0.691 \pm 0.008$$

These results still demonstrated a time resolution that is less than ideal. They also raise the question: why does a different crystal result in better time resolution? I hypothesized that perhaps the photocathode in the second crystal-PMT

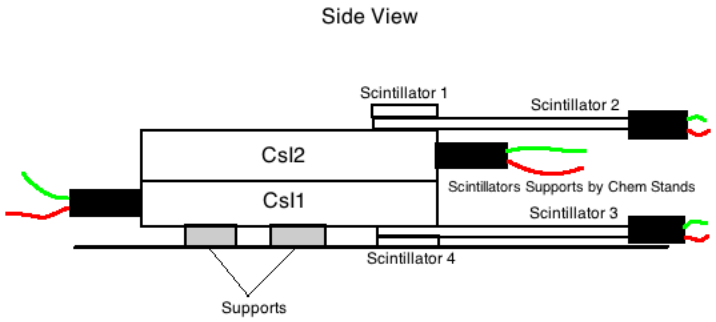

Figure 11: Two Crystal Setup with Muon Track Near to PMT

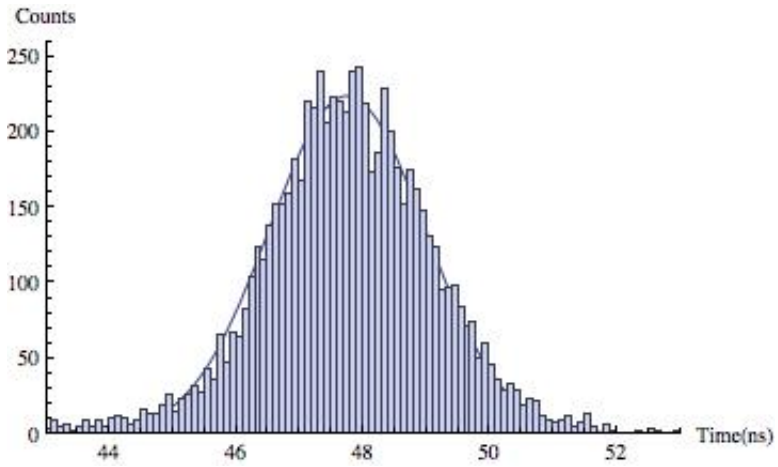

Parameter (units)	Fit Estimate	Standard Error
Amplitude a (counts)	689	8
Mean μ (ns)	47.745	0.017
Standard Deviation σ (ns)	1.229	0.017

Figure 12: Histogram of Pulse Times for Two Crystal Setup with Muon Track Near to PMT and Fit Statistics

combination was more efficient and therefore produced more photoelectrons per MeVof deposited energy.

The reason the number of photoelectrons, $n_{p.e}$, affects the time resolution stems from the fact that the time between when a photon hits the photocathode and when an electron is ejected has a small degree of variability. The more photoelectrons that are ejected, the closer the average time delay between photon arrival and electron ejection will be to the expected value. Therefore, more photoelectrons per pulse means less random variability in time between pulses and more regular pulse shaping.

Therefore, I decided to calculate the average number of photoelectrons per pulse for the two crystals. I used the following relation

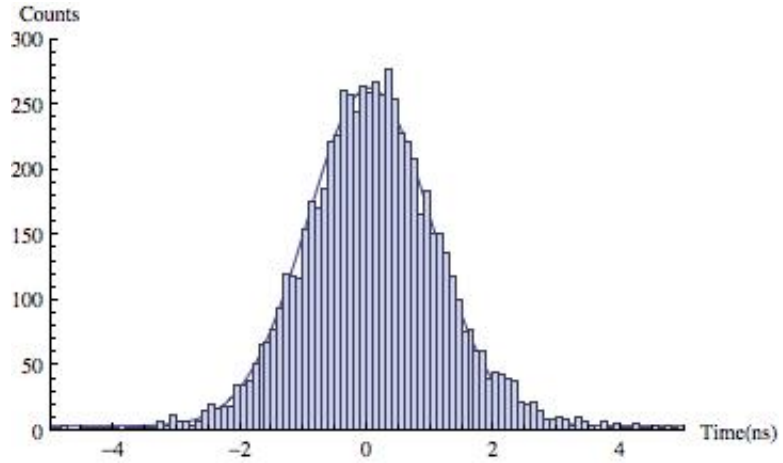

Parameter	Fit Estimate	Standard Error
Amplitude a (counts)	634.6	7
Mean μ (ns)	0.031	0.009
Standard Deviation σ (ns)	0.977	0.011

Figure 13: Histogram of Pulse Times for CsI Crystal 3

$$\bar{n}_{p.e} = \left(\frac{\bar{E}}{\sigma_E}\right)^2$$

The area under the curve of each pulse should be proportional to the total energy of the pulse. Therefore I calculated the energies of the ADC pulses by integrating the fitted gaussian function. Then I plotted the results in a histogram, which is presented below.

$$\bar{n}_{p.e_{C1}} = \left(\frac{\bar{E}}{\sigma_E}\right)^2 = \left(\frac{15610.6}{3406.8}\right)^2 = 21.0$$
$$\bar{n}_{p.e_{C2}} = \left(\frac{\bar{E}}{\sigma_E}\right)^2 = \left(\frac{10203.1}{1620.7}\right)^2 = 40.1$$
$$\bar{n}_{p.e_{C3}} = \left(\frac{\bar{E}}{\sigma_E}\right)^2 = \left(\frac{11403.6}{1634.8}\right)^2 = 48.7$$

First, we should notice that the pulse energies follow the Landau distribution which is expected because the muons are depositing energy via Bremmstrahlung radiation. When calculating $\bar{E}$ and σ_E I considered only the data contained within the symmetric region of the peak because this is the area governed by Poisson statistics.

As hypothesized, CsI 3, the crystal with better time resolution also had more photoelectrons per pulse on average.

To further establish the relationship between a high number of photoelectrons and better time resolution, I created a histogram of pulse times from Crystal 3 , only including thoses pulses with energy greater than 20,000 units. The cutoff 20,000 units was selected because pulses with energies above this cutoff had energies well above the mean energy, but the cutoff was not so high that our fit statistics from the resultant histogram would have too much uncertainty to be meaningful. The results are presented below.

$$\sigma = 0.847 \pm 0.021.$$

$$\sigma_{CsI} = \frac{\sigma}{\sqrt{2}} = \frac{0.847}{\sqrt{2}} = 0.599$$

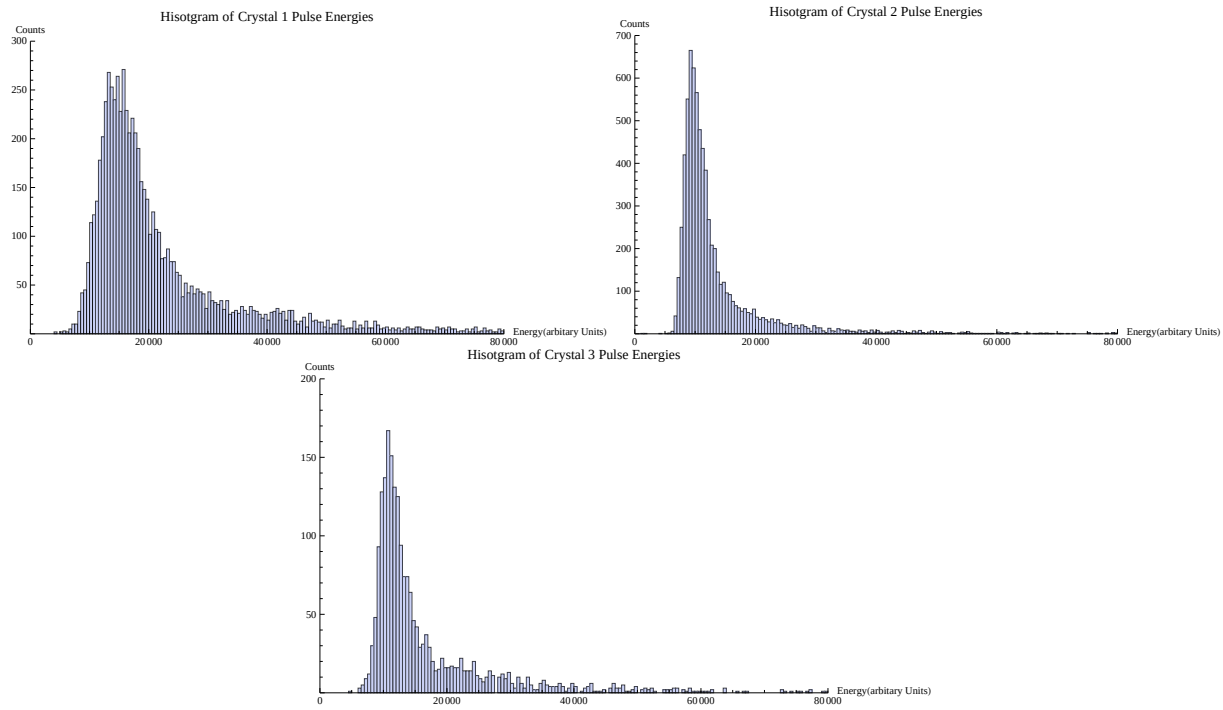

Figure 14: Histograms of Pulse Energies for Crystals 1-3

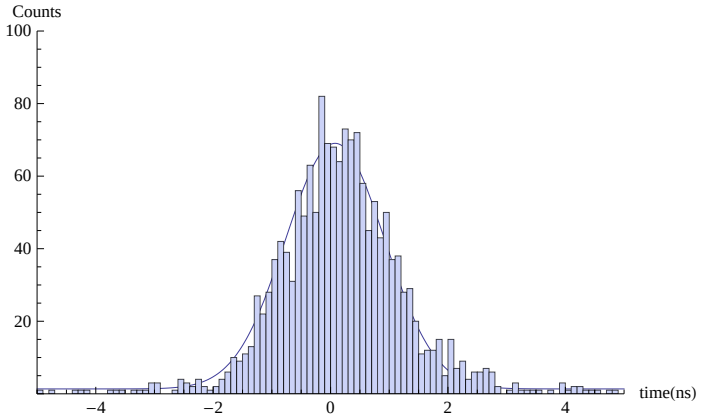

Parameter	Fit Estimate	Standard Error
Amplitude a (counts)	143	4
Mean μ (ns)	0.077	0.018
Standard Deviation σ (ns)	0.847	0.02

Figure 15: Histogram and Fit Statistics for Pulses with Energy Greater than 20,000 Units

$$\Delta\sigma_{CsI} = \frac{\partial\sigma_{CsI}}{\partial\sigma}\Delta\sigma = \frac{0.021}{\sqrt{2}} = 0.015$$

so,

$$\Delta\sigma_{CsI} = 0.599 \pm 0.015$$

When looking at only the highest energy muons the time resolution improved by approximately 0.1ns. The mean error in the mean time resulting from the fit is 0.19ns for these higher energy pulses, indicating that pulses made of more photo-

electrons are reshaped to more perfect gaussian than lower energy pulse. Clearly the low total number of photoelectrons contributes strongly to the time reoslution. The idea that lower energies pulses have worse time resolution is not new. However, we should note that the variability in photoelectron statistics between crystals can create a difference in time resolution even for events that have the same energy.

The gammas that make up the golden decay signal will be on the order of 100MeV. Each of these gammas should produce approximately 40-100 photoelectrons per MeV. This 100-fold increase in $n_{p.e}$ should greatly reduce the limit in time resolution that photoelectron statistics seem to be imposing on our muon measurements.

The spatial resolution of our experiment inserts another source of timing uncertainty. Up until this point I have assumed that all of the cosmic muons have followed the same exact track through the detector and therefore the time between when the pulse from CsI 2 arrives and when the pulse from CsI 1 arrives should be the same for all muons. We have assumed that the only variation in the difference between these measurements is due to imperfect time resolution. However, in reality there is some spatial variation in muon trajectory that produces variation in timing that is real and not a product of imperfect resolution. In order to collect any data our detector must have a nonzero solid angle of muon acceptance. If muons pass through the detector at an angle to the vertical then they pass through one crystal closer to the PMT than they do through the other. Therefore the time it takes the photons from one crystal to arrive at the PMT is shorter than for the second crystal, because the distance the light must travel before measurement is smaller. Therefore the difference between t_{CSI} and t_0 will be slightly different if the muon passes through the detector at an angle than if it travels perfectly perpendicular to the table.

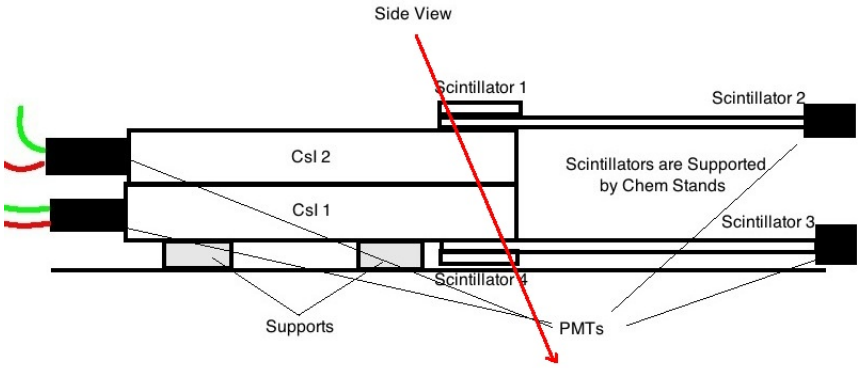

Figure 16: Illustration of How Muon Angle Could Introduce Variation in Pulse Times

The speed with which the light travels through the crystal is a function of the index of refraction of the material. Cesium-Iodide has index of refraction $n = 1.79$. We can use this value and the speed of light c to calculate v.

$$v = \frac{c}{n} = \frac{3 \times 10^8 \mathrm{m/s}}{1.79} = 1.68 \times 10^8 \mathrm{m/s}$$

The time it takes the light to travel the distance d from the muon track to the PMT is

$$t = \frac{d}{v}.$$

Since,

$$t = t_{CsI} - t_0,$$

the variation in t that is introduced by the angular acceptance of the detector is,

$$\Delta t = \frac{\Delta d}{v}$$

where Δd is the different in light path length between CsI 2 and CsI 1. Δd is function of the detector geometry. The most extreme angle to the verticle that the muon can take while still passing through all four plastic scintillators is

$$\theta = arctan(0.1\text{m}/0.2\text{m}) = 0.40\text{radians}$$

When the angle between the muon path and the vertical is at the largest allowable value

$$\Delta d = 0.05\text{m}$$

Therefore angular variation can add a timing error of plus or minus

$$\Delta t = \frac{\Delta d}{v} = \frac{0.05\text{m}}{1.68\times10^8\text{m/s}} = 0.30\text{nm}.$$

In order to reduce this error due to spatial uncertainty, I reduced the overlap of the plastic scintillators as shown below to reduce the accepted solid angle.

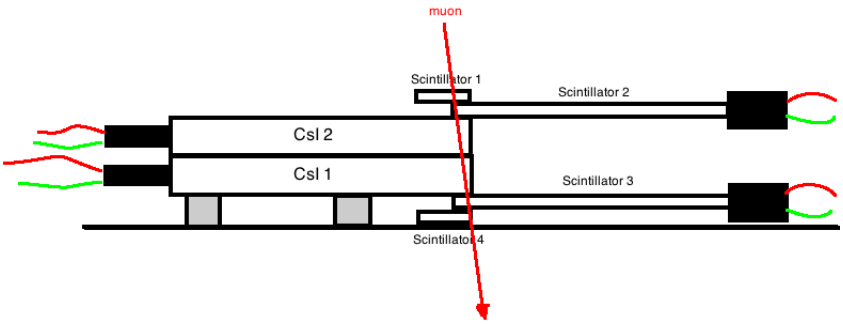

Figure 17: Revised Setup, with Less Scintillator Overlap, Designed to Reduce Angular Acceptance

With this reduced overlap the rate of data taking was extremely slow (roughly 1 hit per half hour). I took data over the course of two weeks. However, the VME experienced an error twice during the course of these two weeks and data taking stopped for 2 days each time before this was noticed and fixed. In the end the volume of data was small, which greatly increases the uncertainty of the results compared to the other data sets. First we must note that this data was taken with crystal 2 (crystal 1 was used to define t_0 as always). When comparing the time resolution to the two other sets of data from crystal 2 we see an encouraging drop in the estimate time resolution. $\sigma = 1.01 \pm 0.13ns$ compared with $\sigma = 1.196 \pm 0.020$. and $\sigma = 1.229 \pm 0.017ns$. The difference is statistically significant although the regions of error are near to overlapping. I suspect that more data could demonstrate this trend more strongly.

This gives,

$$\sigma_{CsI} = \frac{\sigma}{\sqrt{2}} = \frac{1.01}{\sqrt{2}} = 0.72 \; \Delta\sigma_{CsI} = \frac{\partial\sigma_{CsI}}{\partial\sigma}\Delta\sigma = \frac{0.13}{\sqrt{2}} = 0.09$$

The time resolution is $\sigma_{CsI} = 0.72 - 0.09$.

5.4 Conclusions

The standard conversion for muon energy deposition is 2MeV deposited per cm of scintillator traversed. The muons traveling through the two crystal setup have a minimum path length of 10cm (the height of the crystal) and a maximum path length of 12.2cm in each crystal. We expected the mean energy deposited to be approximately 20 MeV. Therefore we expect the time resolution to be better than 0.5ns which is the expected time resolution for 10MeV. The

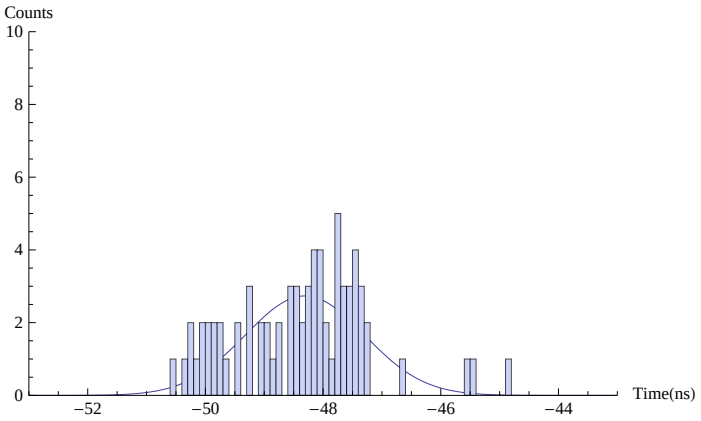

Parameter (units)	Fit Estimate	Standard Error
Amplitude a (counts)	6.9	0.8
Mean μ (ns)	-48.31	0.13
Standard Deviation σ (ns)	1.01	0.13

Figure 18: Histogram and Fit Statistics from Reduced Overlap Setup

best time resolution we measured is $0.599 \pm 0.015\text{ns}$ and this is only when restricting our attention to the higher energy muons (with a mean energy that is likely greater than 20MeV). The discrepancy between the predicted and the observed time resolution is partially due to uncertainty in position. Reducing the scintillator overlap created a 0.1ns drop in σ_{CsI}. This source of uncertainty is an artifact of how we chose to measure time resolution, by assembling "identical" events and characterizing their time spread. This is an error in our assumptions about the identical nature of the events and not error in measurement. This source of error will not effect the time uncertainty of actual KOTO events.

Also, our method for predicting the ideal time resolution is imprecise. We predict the muon events will have a mean energy of 20MeV and therefore 0.5ns, the predicted time resolution for 10Mev, is a safe upper bound. However, the 2MeV per cm heuristic that we used to make this prediction is proven to be accurate for plastic scintillators. We are using CsI scintillators not plastic scintillators. A study on muon energy loss in CsI would be necessary to determine the actual mean energy deposited.

Lastly, we must take note of the variation in photoelectrons per MeV for the CsI crystals used in this experiment. The mean number of photoelectrons varied by up to a factor of two between crystals. Because the crystals were observing the same cosmic background this indicates that photoelectrons per MeV can vary by up to a factor of two between crystals. As we demonstrated, this variation can cause variation in time resolution between crystals. We observed a 0.15ns difference in time resolution between crystals due to this effect. This has important implications for the KOTO CsI array. The photoelectrons per MeV for each block should be measured individually in order to truly understand calorimeter performance.

5.5 References

[1] J. Ma, et al., The Bessel Filter Simulation (2007)
[2] Comfort et al., Proposal for $K_L \to \pi_0 \nu \bar{\nu}$ Experiment at J-Parc (2006)